Spin Transport in Graphene

Minkang Li

Master of Science by Research

University of York

Physics, Engineering and Technology

January 2024

Abstract

Graphene is a material with a special electronic structure and conductivity properties. It exhibits some unique phenomena and potential applications in spintronics. Because its spin orbit interaction is very small, and carbon has almost no nuclear magnetic moment. Studying how to achieve spin injection and spin transport in graphene is a key direction in spintronics. This study investigates the spin injection and spin diffusion lengths in graphene.

Firstly, some hemispherical permalloy dots were fabricated on graphene using photolithography technology and sputtering system for spin injection and spin diffusion lengths measurements. Hemispherical shape can minimize the influence of magnetic anisotropy and enable us to check if there are any differences in spin diffusion length based on the magnetic field angle. Obtaining the spin diffusion length of graphene at room temperature through non local measurements and spin Hall effect.

CONTENTS

Acknowledgements

I would like express my gratitude to all the people who helped me during my experiments and completing my thesis.

First of all, I would like to express my gratitude to my supervisor Professor Atsufumi Hirohata. He is the most patient and kind teacher I have ever met. He helped me choose my research direction and gave me many good suggestions in experimental design and thesis writing. I am very grateful for his help and guidance.

Secondly, I would like to express my gratitude to the PhD students Alex and Erion who share the same office as me, as well as visiting scholar Dr. Wei Li. They provided a lot of help during my experiments using clean room equipment. And also our cleanroom supervisor Charan,

My other supervisor, Dr. Andrew Pratt, has also provided me with great assistance in my research.

Finally, I would like to thank my family and friends for their support, concern, and trust in me.

Declaration of Authorship

I declare that this thesis is a presentation of original work and I am the sole author. This work has not previously been presented for a degree or other qualification at this University or elsewhere. All sources are acknowledged as references.

1. Introduction

1.1 Research Background

Electrons have two important properties, a charge and a spin.[1] Modern microelectronics technology mainly utilizes the charge of electrons since the 19th century, developing microelectronics based on semiconductors and laying the foundation for the third industrial revolution. [2] However, with the continuous development of the semiconductor technology and the continuous reduction of transistor size, further technological breakthrough faces increasing challenges. The major difficulty is the increased manufacturing processes, and the requirement of large capital investment for equipment and technology to be used to manufacture next-generation chips, resulting in high device costs.[3] From research and development to production, a long-term cycle is required. At the same time, as chip size continues to shrink and the corresponding performance improves, the power consumption and Joule heating of integrated circuits also continue to increase.[4] These factors constrain the production and development of the semiconductor industry.

Therefore, utilizing the spin properties of electrons to develop new electronic devices has been attracting broad interests. Spintronics, as a new interdisciplinary field in condensed matter physics, will become one of the core technologies of the next round of information industry revolution.[5]

Spintronics mainly studies the processes closely related to an electronic charge and spin, including spin generation, injection, transport, detection and control, ultimately achieving new types of electronic devices.[6] The research and development to achieve them have become a hotspot of common interests in many fields, not only condensed matter physics but also information technology and materials science, and will play a crucial role in the future development of the electronic industry. The semiconductor devices, which are the basic elements of modern information industry, carry information using the charge characteristics of electrons (or holes), while electron spins, due to its random orientation, do not carry information. [7] Spintronics utilizes not only charges, but also spin properties of electrons for data processing as well. With the development of microfabrication technology and large-scale integrated circuits, the size of electronic devices is becoming smaller and smaller. When the scale is in the nanometer range, a spin is superior to a charge in many aspects, such as fast data

processing, low energy consumption, high integration, and good stability. These characteristics can also solve the Joule heating and scalability problems caused by the miniaturization of the above-mentioned electronic devices to a certain extent.[8] Therefore, spintronics will gradually replace microelectronics and become the mainstream of industry.

1.2 Graphene

Graphene is a novel two-dimensional material composed of single layer carbon atoms. Its shape is similar to a honeycomb shaped hexagonal. Carbon atoms have four valence electrons, three of them form sp^2 bonds. [9] Carbon atoms share unbound electrons with its three adjacent carbon atoms to form π bonds. The structure of graphene is very stable, with a carbon-carbon bond of only 1.42×10^{-10} m. The connections between carbon atoms inside graphene are very flexible. When an external force is applied to graphene, the surface of the carbon atoms will bend and deform, so that the carbon atoms do not need to rearrange their arrangement to absorb the external force, thereby maintaining structural stability. This stable lattice structure gives a graphene excellent thermal conductivity. In addition, electrons in graphene do not get scattering due to lattice defects or the introduction of foreign atoms when they move in their orbits. Due to its strong interatomic forces, at room temperature, even if the surrounding carbon atoms collide, the interference on electrons in graphene is very small.

The special structure of a graphene make it has extremely high electric conductivity, thermal conductivity, mechanical strength, and chemical stability.[10]
A graphene is also one of the best conductive materials in the world. Table 1.1 shows the resistivity of various materials at 20℃. The electrical resistivity of a graphene at 20℃ is nearly 60% lower than the most conductive metal, silver.

Table 1.1. The resistivity of various materials at 20℃.

Material	**Resistivity ρ(Ω·m) at 20℃**
Graphene	$1.00x10^{-8}$
Silver	$1.59x10^{-8}$
Copper	$1.68x10^{-8}$
Gold	$2.44x10^{-8}$
Aluminium	$2.82x10^{-8}$

Notes: Data sourced from Baidu. (https://baike.baidu.com/item/%E7%94%B5%E9%98%BB%E7%8E%87/786893?fr=ge_ala)

Meanwhile, a graphene also has the highest thermal conductivity. Table 1.2 shows the thermal conductivity of various materials. The thermal conductivity of a pure defect free monolayer graphene reaches up to 5300W/m·K.[11]

Table 1.2. The thermal conductivity of various materials.

Material(solid)	**Thermal conductivity (W/m·K)**
Graphene	4840-5300
Carbon nanotubes	3000
Silver	420
Iron	80
Glass	1

Notes: Data sourced from Baidu. (https://baike.baidu.com/item/%E7%83%AD%E5%AF%BC%E7%8E%87/868266?fr=ge_ala)

A graphene is one of the materials known to have the highest strength, good toughness and high bending resistance. The theoretical elastic modulus of a graphene reaches 1.0 TPa, and the inherent tensile strength is 130 GPa.[12]

The carrier mobility of a graphene at room temperature is about 15000 $cm^2/(V·s)$, which is more than 10 times larger than that of silicon and more than twice larger than that of indium antimonide (InSb), which is known as the conventional material with the highest carrier mobility. Under certain specific conditions, such as low temperature, the carrier mobility of a graphene can even reach up to 250000 $cm^2/(V·s)$. Unlike many other

materials, the electron mobility of a graphene is less affected by temperature changes. At any temperature between 50-500K, the electron mobility of a single-layer graphene is around 15000$cm^2/(V \cdot s)$ in the ideal condition.[13]

Due to these various excellent properties of graphene, the discovery of a graphene in 2004 has attracted widespread global attention, and scientists have become enthusiastic about exploring its application prospects in various fields. Andrei Geim and Konstantin Novoselov, physicists at the University of Manchester in the UK, won the 2010 Nobel Prize in Physics for successfully separating a graphene from graphite (in 2004) and discovering the integer quantum Hall effect in single-layer and double-layer graphene systems and the quantum Hall effect at room temperature (in 2009).
Among them, the application prospects of graphene in the field of electronics are particularly noteworthy. Its high conductivity and low resistance performance make it have good potential for application in electronic components, becoming one of the key materials for the future electronic technology revolution.[14]

1.3 Spin Injection

In the field of spintronics, a graphene is considered as an ideal medium to carry spins due to its abovementioned unique electronic structure and excellent electron transport performance.[15]

A graphene is not intrinsically spin polarized, and injecting a spin into graphene efficiently is one of the key issues in the field of spintronics. To achieve this goal, special techniques and methods are required as listed in the following:

(i) Spin current injection: By introducing spin polarized current into a graphene, a spin can be injected into a graphene. This is usually achieved by generating a spin polarized current in magnetic materials attached to a graphene, and then transferring it to a graphene. By forming specific structures between a graphene and the other materials or layers, these structures can achieve the transmission and transfer of spin states. For example, the special interface between a magnetic material and a graphene may facilitate the transfer and injection of a spin.[16]

(ii) Magnetic field application: By applying an external magnetic field or utilizing a

magnetic material, electrons or holes injected into a graphene can exhibit spin polarization. These spin polarized charge carriers can carry the spin polarization in a graphene.[17]

(iii) Optical methods: Optical methods can be used to introduce spin polarization, such as using a specific wavelength of laser to manipulate a spin state in a graphene. This requires precise optical control technology.[18]

At present, research in this area is still ongoing and more experiments and technological developments are needed to achieve efficient spin introduction.

1.4 Spin Measurement

Measuring spin transport in a graphene can provide a deeper understanding of the behavior of electron spins in this material, which is of great importance in spintronics and the development of new electronic devices. By measuring the transport of spins in a graphene, we can understand the transport mechanism, velocity and characteristics of spin states in this special material.[19] These characteristics can provide a guidance for the development of new devices such as spin logic gates and spin memory.

Studying the spin transport in a graphene also helps to improve the theoretical foundation of spintronics. Therefore, the significance of measuring spin transport in a graphene lies in again providing important scientific basis and technical support for the development of spintronics and the design of new devices.

Although efficiently achieving the spin transport in a graphene is a challenging task, there are several methods that can be used to study and measure the spin transport in a graphene:

(i) Hall effect measurement: The spin Hall effect is a method to measure the spin transport by applying a magnetic field perpendicular to the direction of a current flowing in a graphene. By measuring the vertical voltage between the current and the magnetic field, information related to the spin transport can be obtained.[20]

(ii) Measurement of valley polarization: The energy band structure in a graphene includes four energy band valleys, which can generate valley states at the minimum of the energy band. Valley polarization is a phenomenon closely related to an electron spin. By controlling the band structure of a graphene or utilizing an external electric field, valley polarization can be measured and the properties of the corresponding spin transport can be controlled.[21]

(iii) Magnetoresistance measurement: Changes in a spin state may lead to changes in magnetoresistance (MR). Usually, by sandwiching a non-magnetic thin film with two ferromagnetic layers, the spin direction of electrons in the magnetic layer is affected by the external magnetic field. If the magnetic moments of two ferromagnetic layers are parallel, electrons are usually more likely to pass through the non-magnetic layer, resulting in lower resistance. If the magnetic moment direction is antiparallel, electron transfer is hindered and resistance increases. This phenomenon causes a significant change in the junction resistance under a magnetic field changes. By measuring the MR in a graphene, the properties of spin transport can be evaluated.[22]

(iv) Laser spectroscopy: Under an external magnetic field, using a laser light source to excite the material and measure its absorption and scattering of light. Due to the coupling between a spin and an external magnetic field, the spectral response unique to a material is affected by the spin state. Magneto optical spectroscopy can provide information on spin.[23]

(v) Measurement of spin valley resonance frequency: By placing a sample in a strong magnetic field, an electron spin magnetic moment can be oriented along the direction of the magnetic field. By applying an external microwave field to induce electron resonance. After the end of microwave lasing, the electron spin begins to freely induce rotation in the magnetic field, producing a change in a magnetic field. By detecting changes in the induction signal, information about the spin of the measured electron can be obtained. The generated spectrum represents the signal intensity at different resonance frequencies of the microwave, forming an electron spin resonance spectrum. The spectrum provides information about the spin state of electrons.[24]

These methods are not all complete on its own, and researchers may need to use multiple techniques to study spin transport in a graphene. There are still many

challenges, such as improving their measurement sensitivity, controlling impurities, etc. in order to obtain a deeper understanding and precise controllability of the spin transport properties in a graphene.

1.5 Spin Valves

A graphene spin valve is a graphene based device used to control the spin flow, similar to a transistor in conventional electronics. It can regulate the flow of spins and achieve information processing.[25]

A graphene spin valve typically forms a structure consisting of a graphene and two ferromagnetic electrodes. The working principle relies on controlling spin injection and flow, injecting spin polarized carriers into a graphene through a ferromagnetic electrode, so that electrons or holes in a graphene have a specific spin orientation. [26] Using an external electric field, magnetic field, or the other controling methods, the direction or density of spin flow can be modified, thereby achieving the control over spin information. A graphene spin valve may also include an isolation layer to isolate spin flow and prevent spin information from spreading in unwanted areas.

The research on a graphene spin valve aims to solve the problems of information control and process in spintronics, providing potential solutions for the development of new spintronic logic and memory. Although research on a graphene spin valve is still on its early stages, it represents a promising device concept. Drögeler *et al.* used Co as a spin injector, MgO as a tunneling layer, and encapsulated the electrodes with hBN. The corresponding spin relaxation time was measured to be on the order of nanoseconds for a mechanically exfoliated graphene, resulting in a spin diffusion length to be 10 μm. [27] By increasing the packaging area of hBN, the spin relaxation time was further increased to 12.6 ns, leading to the spin diffusion length of 30.5 μm.[71]

As a chemical vapor deposition (CVD) method for producing a graphene has gradually matured, mass production of spin valves has become possible. The CVD is a method of growing a graphene on a metal substrate through gas-phase chemical reactions. Usually at high temperatures, a graphene is deposited on a metal surface by heating a metal substrate (such as copper and nickel) and exposing it to a carbon source gas (such as methane). [28] This method can produce large areas of a graphene, so it is commonly

used in applications such as electronic devices and transparent conductive films. Avsar *et al.* prepared single-layer and double-layer graphene spin valves with a length of 1.15 μm fabricated by copper based CVD. The spin accumulation signal in a single-layer graphene was reported as high as 4 Ω, with a length of 1.35 μm. The spin accumulation signal of a double-layer graphene was about 0.15 Ω. [29]

Although there have been many reports on a graphene as a spin carrier, there are still issues in precisely determining its electrical resistivity, spin lifetime, spin diffusion length, spin Hall angle, spin signal and contact resistance with other materials. At present, there are significant differences in the data obtained from different experiments, and the cause of the differences are not yet clear. In addition, theoretical work is relatively lacking. These issues have been affecting the application of a graphene in spintronics and require further in-depth research.

2. Fundamentals

2.1 Graphene structure

Most of the special properties of graphene are determined by its π bonds. Each carbon atom has a π bond, which covalently combines with neighboring carbon atoms to form π - and π * bands. The band dispersion relationship of graphene can be calculated using a tightly binding approximation model,[30] as shown in Figure2.1[31]. The upper π * band is the conduction band, and the lower π * band is the valence band. Due to the presence of two carbon atoms in each crystal cell of graphene, each contributing one electron, the π - band of graphene is precisely filled with electrons, while the π * band is empty. Therefore, the Fermi surface of graphene lies between the π - and π * bands, and intersects at the K (K ') point in the Brillouin zone, exhibiting a semi metallic property of zero band gap. Due to the fact that electrons located near the K (K ') point no longer follow the traditional Schrödinger equation and can only be described using an equation likes Dirac equation, the K (K') point is also known as the Dirac point. Near point K, the stationary effective mass of an electron is 0, and its Fermi velocity can reach 10^6 m/s, which is 1/300 of the speed of light.[32]

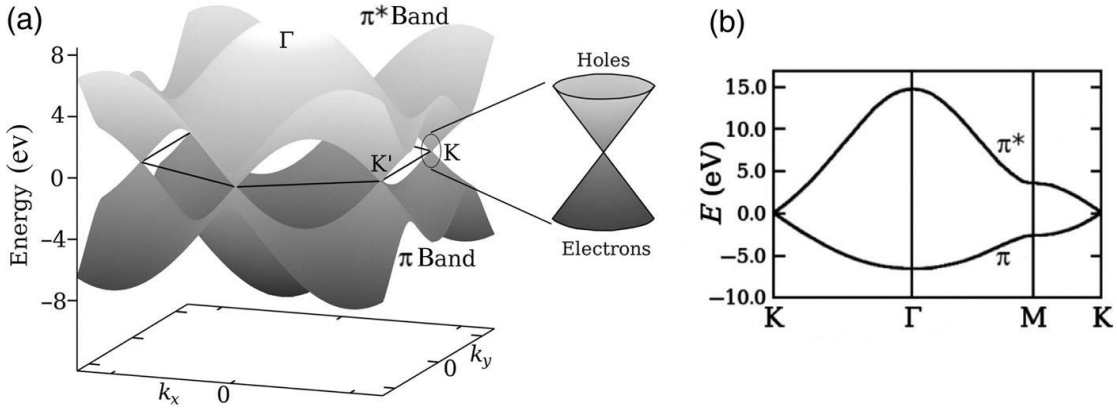

Figure2.1. (a)Energy dispersion relation for graphene. (b)The dispersion along the high-symmetry points ΓMK.
Notes: Isotopical Band - Gap Opening in Graphene(2016)

The number of layers and stacking method of graphene can both affect its electrical properties. Single layer graphene exhibits a semi metallic property with a zero bandgap structure. At room temperature, its carrier migration is 15000 $cm^2/(V \cdot s)$, and its resistivity is only 1.00×10^{-8} Ω·m. This low resistance value and high mobility

performance make graphene suitable for ultra-thin and fast electronic devices.[33,34] For double-layer and multi-layer graphene, the stacking method between layers determines their electronic structural characteristics. The double-layer graphene stacked with AA also exhibits zero bandgap and metallic properties, while the double-layer graphene stacked with AB (half of the carbon atoms in the second layer of graphene are located at the center of the first layer of hexagonal ring) will open the bandgap under the control of a transverse electric field, exhibiting semiconductor properties.[35] Similarly, with zero bandgap, the electron energy dispersion of single-layer graphene is different from that of AB stacked double-layer graphene, with the former exhibiting a linear dispersion (Figure 2.2 a) and the latter exhibiting a parabolic distribution (Figure 2.2 b). After applying an electric field, the bandgap opens, and the size of the bandgap opening can be adjusted by the electric field (Figure 2.2 c). [36] This adjustable band structure provides many possibilities for the application of graphene.[37]

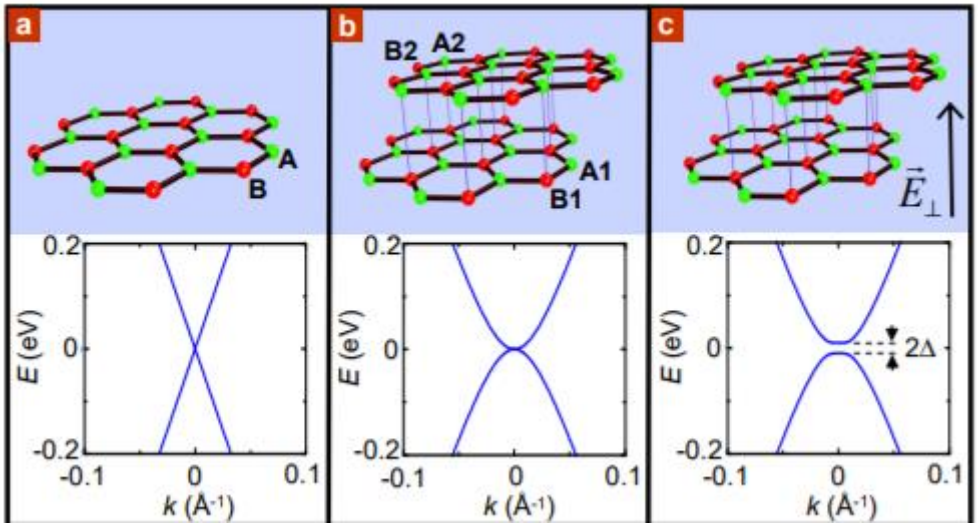

Figure2.2. (a) diagram of single-layer graphene lattice structure and energy dispersion. (b) diagram of double-layer graphene lattice structure and energy dispersion. (c) diagram of double-layer graphene bandgap opening after applying a vertical electric field and energy dispersion.

Notes: Gate-induced insulating state in bilayer graphene devices(2008)

2.2 Spin transport

Spin transport is a mode of electron transport, and it is the most fundamental concept in spintronics. The transport phenomenon discusses the transport of charges and energy under the influence of electric fields, magnetic fields, temperature fields, and other

factors.

The study of spin transport is an emerging field that has attracted the attention of many scientists in the past few decades. Theoretical and experimental research have achieved many important results, promoting the development of spintronics and providing a key foundation for the design and application of new spintronic devices.

The earliest observed electron spin related phenomenon is generally believed to be the anisotropic magnetoresistance effect discovered in 1857,[38] which means that below the Curie temperature, the resistance of ferromagnetic materials changes with the relative orientation of current and magnetization in the material. The magnitude of anisotropic magnetoresistance is defined as the ratio of the difference in resistivity between the applied magnetic field and the direction of current parallel and perpendicular to the average resistivity. For Fe or Co materials, the anisotropic magnetoresistance value is approximately 1%.[39] The microscopic mechanism of anisotropic magnetoresistance is spin dependent scattering caused by electron spin orbit coupling.[40] In 1986, German scientist Grunberg and his research team discovered antiferromagnetic exchange coupling between adjacent ferromagnetic layers in Fe/Cr/Fe multilayer films. [41] Fert and his research team found a magnetic resistance change rate of up to 100% in Fe/Cr superlattice systems prepared using molecular beam epitaxy, which is much higher than the previously observed anisotropic magnetic resistance change rate, hence it is called the giant magnetoresistance effect. Subsequently, Parkin used magnetron sputtering to prepare Cr/Cu superlattices, and also observed a giant magnetoresistance value of 115% in the Cr/Cu superlattice. [43] However, there is a strong interlayer exchange coupling effect in magnetic multilayer films, which usually requires an external magnetic field of more than 1T to reach saturation, reducing the sensitivity of magnetic multilayer films and hindering their application. To address this issue, researchers have proposed a giant magnetoresistance multilayer structure with a spin valve structure. [42,44] In this structure, one of the two ferromagnetic layers has a large saturation field; The saturation field of the other ferromagnetic layer is very small, which can be reversed under the action of a small external magnetic field, thereby improving sensitivity. Spin transport related phenomena, known as tunneling magnetoresistance effect, have also been observed in magnetic tunneling junctions such as ferromagnetic metals/insulating layers/ferromagnetic metals. Its mechanism is the tunneling effect of spin polarized

electrons, which results in higher magnitudes and sensitivity of magnetoresistance. For example, the sensitivity measured in the Py/Al2O3/CoFe/Py tunnel junction can be greater than 20%/Oe; [45] In CoFe/MgO/CoFe tunnel junctions, a magnetic resistance change rate of~220% can be achieved. [46] The discovery and application of spin valves and tunneling magnetoresistance effects have sparked a trend of spin transport. [47]

For ordinary metals and alloys, the spin up and spin down electrons near the Fermi surface participating in the transport process have equal density of states, and the current during transport is spin depolarized. Therefore, traditional metal theory ignores the spin degrees of freedom of electrons. For ferromagnetic transition metal materials, at the Fermi plane, the density of states of spin up and spin down sub bands in the 3D band of ferromagnetic materials is different. In ferromagnetic transition metals, s electrons are the main charge carriers. Due to the fact that the scattering probability from s electrons to d electrons is proportional to the final density of states of the transition, the scattering probability of spin up electrons and spin down electrons is different, resulting in different currents generated by spin up electrons and spin down electrons. In short, the current in ferromagnetic transition metals is in a spin unbalanced state and is a spin polarized current. Its spin polarization rate P is defined as:

$$P=(n_{\uparrow}-n_{\downarrow})/(n_{\uparrow}+n_{\downarrow})$$

$n_{\uparrow}$ and $n_{\downarrow}$ are the number of spin up and spin down carriers, respectively. Thanks to the discovery and successful application of spin valves and tunneling magnetoresistance effects, Aronov and Pikus proposed in 1976 the idea of injecting spin polarized currents from ferromagnetic transition materials into non-magnetic materials, thereby generating an unbalanced state of spin electrons in non-magnetic materials, and effectively measuring this imbalance state. [48] To achieve spin injection of non-magnetic materials, it is necessary to generate spin polarized currents and corresponding detection methods. So far, several methods for generating spin current have been proposed, such as spin pumping, spin Hall effect, and electrical spin injection.

2.3 Electrical spin injection

The traditional spin electron injection method adopts the injection method shown in Figure 2.3. This method involves injecting current from one of the ferromagnetic electrodes in a spin valve and then flowing out from the other ferromagnetic electrode; Meanwhile, measure the voltage between the two ferromagnetic electrodes. Although

this method can observe changes in spin related electrical signals, in this spin valve, the charge flow and spin polarization current flow in the same circuit, and the measured results are the result of the combined action of the charge flow and spin current, which cannot effectively distinguish between the two currents.

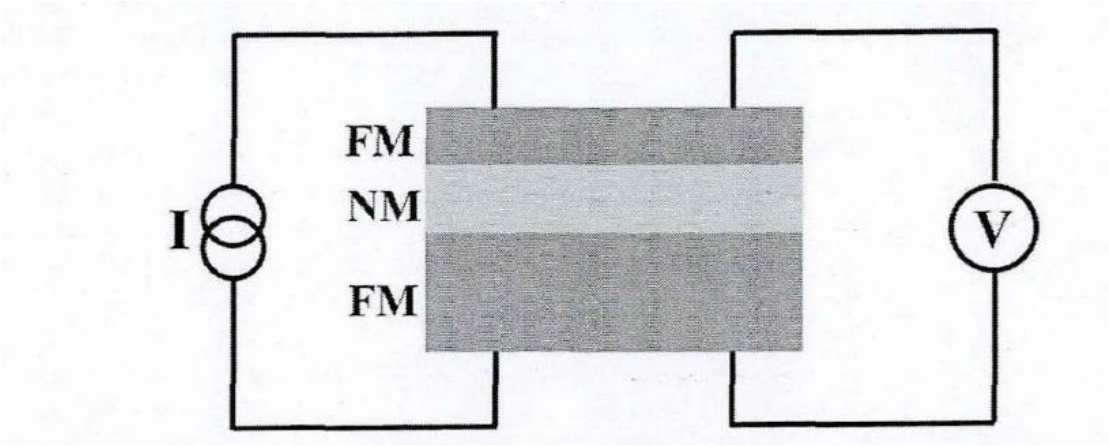

Figure 2.3.Traditional spin valve structure.FM and NM represent ferromagnetic and non-magnetic materials, respectively

In order to obtain pure spin polarized current, researchers proposed a transverse spin valve structure and a non-local method to achieve spin injection and detection. A transverse spin valve has a structure similar to that of a spin valve, where two ferromagnetic materials are isolated by a layer of non-magnetic material, or a non-magnetic strip material is connected to two ferromagnetic strip materials; Formally, it can be seen as spreading the spin valves of traditional stacking onto the surface of the substrate. As shown in Figure 2.4a, on the surface of the substrate, ferromagnetic electrodes F1 and F2 are connected by non-magnetic material N. The injection and detection of spin electrons are achieved using non local methods. As shown in Figure 2.4b, due to the significant spin polarization of ferromagnetic material F1,when a current is applied between the ferromagnetic electrode F1 and the non-magnetic material N, and the current is allowed to flow out from the left side of the non-magnetic material N. After the spin polarized current in ferromagnetic material F1 flows through the interface between ferromagnetic material F1 and non-magnetic material N and enters non-magnetic material N, it will generate an unbalanced state of spin electrons in the non-magnetic material N. This non-equilibrium state will diffuse towards both ends in the non-magnetic material N. The length of this non-equilibrium state in non-magnetic material N is described by the spin diffusion length, and its magnitude can be detected by another ferromagnetic material F2.[49]

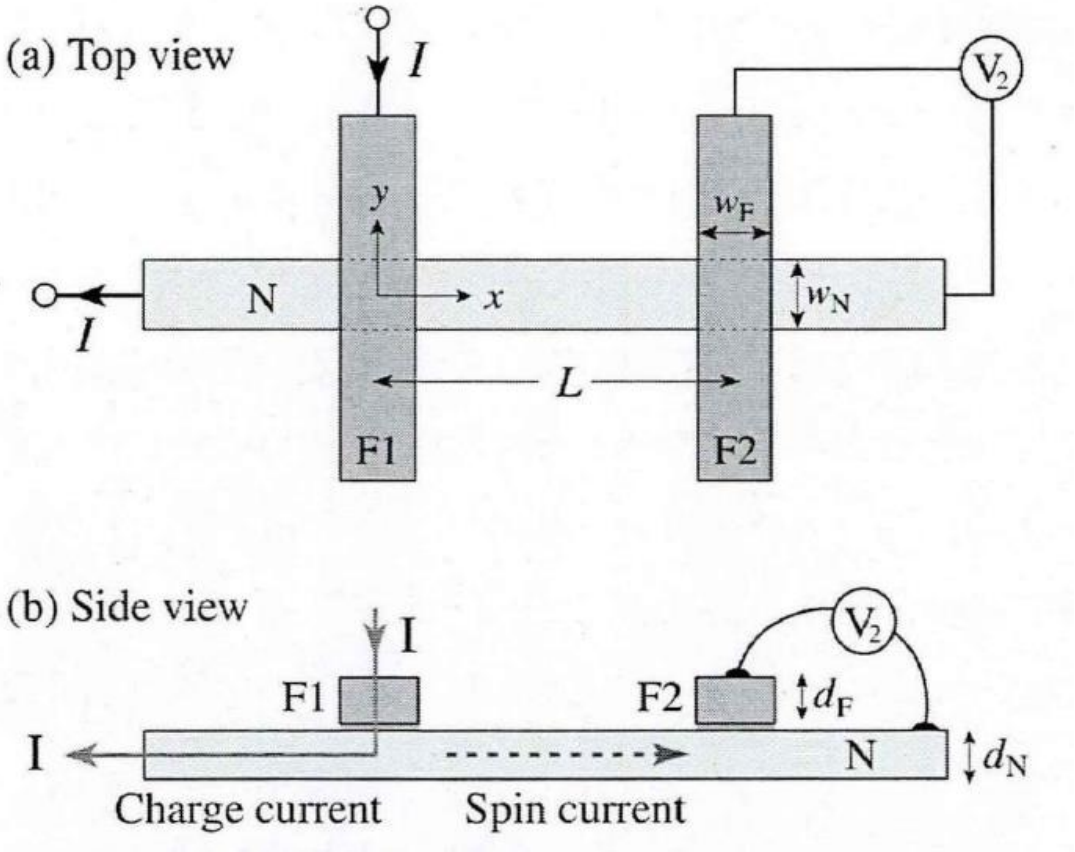

Figure 2.4 Lateral Spin Valve Structure and Non-local Measurement (a)Top vies (b) Side view

Compared with traditional local measurement methods, non-local methods can effectively separate charge flow and spin flow, effectively avoiding the thermal effects caused by current and the effects of anisotropic magnetoresistance. They specialize in studying the effects generated by spin flow. In 1985, Johnson and Silsbee conducted pioneering research on spin injection and detection using lateral spin valve structures and non-local measurement techniques. They used permalloy materials as injection sources for spin electrons and injected spin currents into bulk aluminum. [50] The non-equilibrium strength in aluminum blocks was measured using another permalloy film at low temperatures.

After nearly 20 years of silence, thanks to the advancement of micro and nano processing technology, Jedema successfully achieved spin injection and detection at room temperature. [51] This result has sparked interest in spin injection in transverse spin valves. [52,53] Takahashi et al. investigated spin accumulation in transverse spin valves with different interface combinations. The theoretical results indicate that the spin

accumulation signal in the transverse spin valve with full ohmic contact is the smallest; The spin accumulation signal of the transverse spin valve with an insulating barrier between ferromagnetic and non-magnetic materials is the strongest; When the two interfaces in the lateral spin valve are Ohmic contact and insulation barrier, the spin accumulation signal falls between the two. For these three types of lateral spin valves, their spin accumulation signals decay exponentially with increasing spacing. [54] So far, spin injection of various materials has been studied using a transverse spin valve structure, and experimental results show that when ferromagnetic materials come into direct contact with non-magnetic materials, the spin accumulation signal is generally very small, This is mainly due to the mismatch of spin resistance and spin absorption between ferromagnetic and non-magnetic materials. [55] Introducing a tunneling junction in the transverse spin valve can effectively improve the spin accumulation signal, mainly because the tunneling junction between ferromagnetic and non-magnetic materials can have a high spin polarization rate, [56] which can greatly enhance the spin accumulation signal; However, the high interface resistance of the tunnel junction limits the total current flowing into non-magnetic materials, and the increase in spin accumulation intensity is limited. Fukuma reports that by performing appropriate heat treatment, high spin accumulation signals can be obtained in the transverse spin valve with low interface resistance. Meanwhile, a small interface resistance can ensure the passage of large currents, thereby increasing the strength of spin accumulation. [57]

In most studies, the shape of the electrodes is rectangular. Rectangular magnetic materials may have different magnetic properties along the long and short axes, which can lead to anisotropy. In this study, I consider a new lateral spin valve which have many same hemisphere permalloy dots on the surface of graphene, as shown in Figure 2.5. The spin injection and detection device consist of hemisphere permalloy dots and graphene. Each hemisphere permalloy dots has the same diameter, the distance between adjacent four dots is the same, and there are 7 different distances on a single sample.

Using those hemisphere permalloy dots for injection and measurement so that we don't have any magnetic anisotropy and may also obtain a more uniform current density distribution.

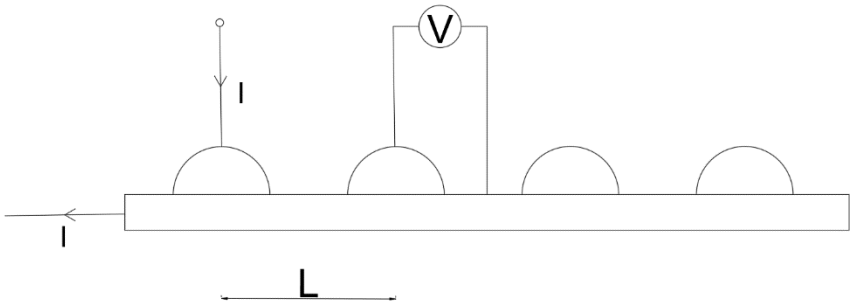

Figure 2.5 New lateral spin valve

2.4 Spin diffusion lengths measurements

Using non local measurement methods to measure the magnitude of spin accumulation in graphene. Inject current into graphene through a permalloy point and flow out from the left side of graphene, while measuring the voltage between the right permalloy point and graphene.

During the measurement process, the magnetization direction of the injection electrode and the detection electrode is controlled by changing the size of the external magnetic field. When the magnetization direction is parallel, a value R_s(U/I) is obtained in units of resistance. When the magnetization direction is opposite and parallel, another unit of resistance, R'$_s$(U'/I), is obtained. The spin accumulation signal ΔR_s is the difference between two measured values.

In order to further understand the spin accumulation in graphene, transverse spin valves with different spacing were prepared, and non-local measurements were performed on each spin valve to obtain their spin accumulation signals. By solving the one-dimensional spin diffusion equation ($R_F \ll R_i \ll R_N$), the expression for the spin accumulation signal and distance is:

$$\mathrm{Rs} = \frac{4P^2}{(1-P^2))^2} R_N \left(\frac{R_i}{R_N}\right)^2 \frac{e^{\frac{-L}{\lambda_N}}}{1-e^{\frac{-2L}{\lambda_N}}} \quad (1)$$

Among them, R_i is the interfacial resistance of graphene/permalloy; R_N is the spin resistance magnitude of graphene; R_i is the spin resistance of permalloy; λ_N represents the spin diffusion lengths of graphene and permalloy respectively; P is the spin polarization rate; L is the center distance between two permalloy electrodes.[54]

By fitting the experimental data with formula (1), the spin diffusion length of graphene at room temperature can be obtained.

2.5 Spin Hall effect

In the 1970s, Dyakonov and Perel[58] theoretically predicted the existence of the spin Hall effect, which means that in materials with spin orbit coupling, there will be a spin current in the lateral direction of the system driven by longitudinal current. This means that electrons with spin up will move towards one side of the sample, while electrons with spin down will move towards the other side of the sample. In a closed circuit system, there will be an accumulation of upward spin at the boundary, On the other boundary, there is an accumulation of downward spin. Currently, the formation mechanism of the spin Hall effect is similar to that of the anomalous Hall effect, so studying the anomalous Hall effect helps to understand the spin Hall effect. The non intrinsic mechanism of the spin Hall effect is believed to be due to spin related skew scattering [59] and lateral jump scattering caused by impurities and vacancies in the crystal, Electrons with spin down and spin up are scattered in opposite directions, respectively. The intrinsic mechanism suggests that it is the intrinsic behavior of the system, without the need for external impurity atoms. The spin orbit coupling and special band structure of the system itself can cause electrons with different spin directions to move in opposite directions. [60]

The anomalous Hall effect (AHE) refers to the transverse voltage that develops in a ferromagnetic material under an applied electric field, even in the absence of an external magnetic field. This effect is generally observed in materials with intrinsic magnetic ordering and is attributed to the spin-orbit coupling and the Berry curvature in the material's electronic band structure.

From the introduction of the anomalous Hall effect in the previous text, it can be seen that in magnetic materials, carriers have the characteristic of spin polarization, and the number of carriers deflected on both sides is different, resulting in the accumulation of both charge and spin; In non-magnetic materials, the number of carrier deflections caused by the spin Hall effect is consistent on both sides, resulting in only spin accumulation and no charge accumulation. Because there is no charge accumulation,

testing the spin Hall effect is very difficult.

30 years after the prediction of the spin Hall effect was proposed, Zhang [61], Murakami[62], Sinova et al. [63] proposed schemes to observe the spin Hall effect in semiconductor materials. In 2004, Kato et al. [64] used the magneto optical Kerr effect to observe the spin Hall effect for the first time in n-type doped GaAs single crystal films. They applied 10 mV longitudinally on the strain free epitaxial GaAs thin film. The electric field of micrometre is such that for carriers with vertical film surface spin, carriers with upward and downward spin will lean towards the left and right sides of the sample, resulting in upward and downward spin potential accumulation at the left and right boundaries. Kato et al. [64] also observed an exponential decay effect of spin accumulation from the boundary to the center in experiments, and the degree of spin accumulation will also increase with the increase of electric field strength, This is also consistent with the image of the spin Hall effect. The experiment also indicates that the self selected diffusion length in GaAs can reach several μ m. However, the phenomenon discovered by Kato et al. was dominated by the non intrinsic spin Hall effect. Subsequently, Wunderlich et al.[65] Observed the intrinsic spin Hall effect in hole type semiconductors using the spin light-emitting diode method. Moreover, in 2005, Kane and Mele[66] and Zhang et al. [67] predicted a quantum version of the spin Hall effect. Two years later, This prediction was experimentally validated by Molenkamp et al. [68] in the CdTe/HgTe/CdTe quantum well system. Subsequently, Fang et al. [69] predicted the existence of a quantum version of the anomalous Hall effect, and Chang et al. [70] soon confirmed the existence of the anomalous quantum Hall effect in 2013.

3. Methodology

This study used photolithography to prepare hemispherical permalloy dots on a graphene. By measuring non-local spin valve and spin Hall effect signals, the spin diffusion length can be calculated. By changing the direction of the magnetic field during the measurement process, the change in the spin diffusion length can be measured. In order to optimize the fabrication process for the permalloy dots, I grew them on silicon substrates using high vacuum sputtering, and imaged them by optical microscopy. The optimized process was used to grow dots on graphene.

3.1 Design of Mask

The first step was to design a mask for the photolithography. The design of the mask is shown in Figure 3.1 .The mask was a 3" chrome photomask. I designed the mask using Autodesk AutoCAD 2023 and asked JD Photo Data to fabricate it. The mask is mainly divided into three sections as follows.

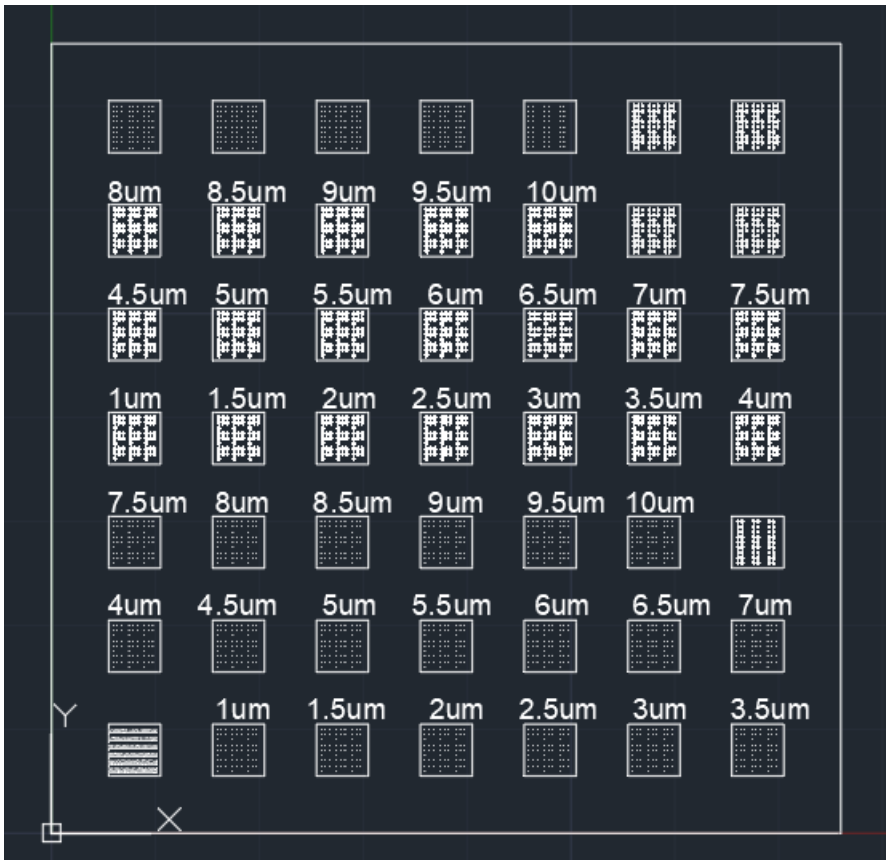

Figure 3.1. The design of the mask

The part inside the square in the bottom left corner of the mask was used to find an appropriate diameter to get the best shape of permalloy dots. The diameter of holes designed on the mask was expected to control the formation and shape of a deposited dots after the deposition and lift-off processes. In the mask, I designed a row of 19 circular holes with different diameters with sequentially increasing from 1 μm to 10 μm by a 0.5 μm step.

The distance between the centers of two adjacent holes was set as 2.0 μm. This section was used to grow permalloy dots on silicon substrates. By observing the shape and radius of the hemispherical permalloy dots by optical microscope, I determined the best diameter (and the growth angle as described in the following section).

Once an appropriate is determined, the second section was used to fabricate permalloy dots on a graphene. The second section had four holes with the same diameter in a row. The distance between the adjacent holes is the same for four holes. However, there are seven sets with different distances with increasing sequentially from 1.8 μm up to 3 μm by a 0.02 μm step. This section was used to deposit permalloy dots on a graphene, to measure non-local spin valve and spin Hall effect signals using four dots for four-terminal measurements.

The third section also had four larger squares that can be connected to the second section. Because the size of the second section is very small, I planned to use this section to help with measurement, but in the end, I did not use the second section for the measurements.

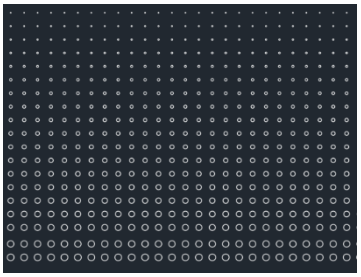

Figure 3.2. The first section of the mask

Figure 3.3. 2.5μm part of the second section

3.2 Design of Bracket

The incident angle between the substrate and the deposition beam has been known to provide a certain impact on the sputtering process. Hence I designed a bracket that allowed me to control an incidence angle for sputtering. The bracket had twelve slopes, each of which had a different angle to the deposition beam. Accordingly, twelve different incidence angles were used for the permalloy growth from 25° to 80°. The design of the bracket is shown in Figure 3.4.

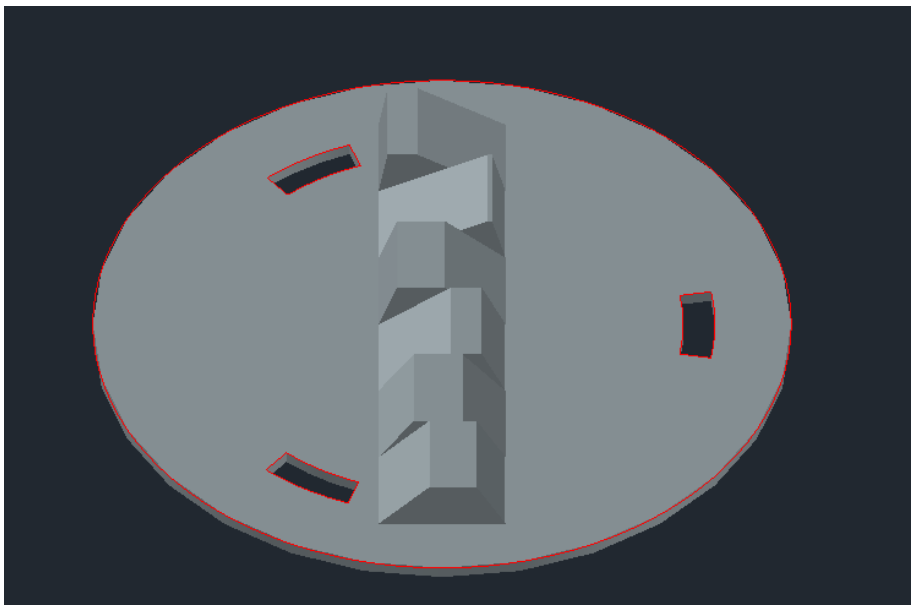

Figure 3.4. The design of the bracket

3.3 Photolithography

The ultrasonic cleaning was used for a substrate with isopropanol for ten minutes. After the ultrasonic cleaning, deionized water was used to clean the substrate, followed by blow dry with nitrogen gas. I then spin coated the photoresist (S1818) with a homogenizer.

Here the rotational speed can affect the thickness of the photoresist . Figures3.5 provides the information required to properly select the speed to achieve the resist thickness needed for the permalloy growth. The best coating uniformity is typically attained between the spin speeds of 3500 and 5500 rpm. Because I want to obtain a hemisphere shape, the thickness of the resist should be longer than the radius of the hemisphere shape, otherwise adjacent dots will be connected during the sputtering. So I selected the speed of 3500rpm for 35 s in this study, allowing me to obtain the thickness of photoresist to be about 2.1 μm.

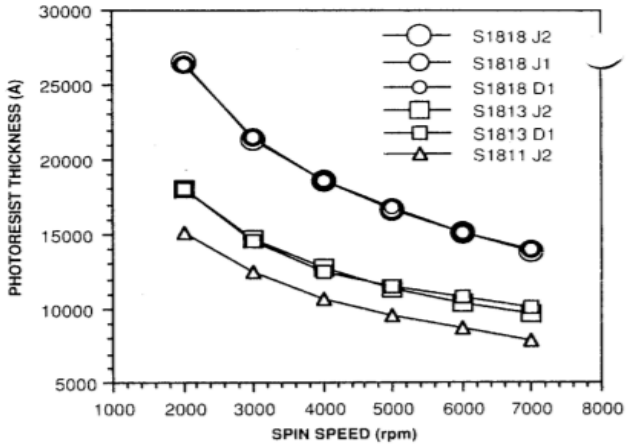

Figure 3.5. Spin speed dependence of photoresist thickness.

After baking at 115°C for 60 s to cure the resist, I placed the sample in the lithography system (UV-KUB3). It has been well known that exposure time and power both have an impact on the patterns made by the lithography. After multiple attempts, I found the best parameter is the power of 70% for 30 s. After exposure, I developed it using the developer (MF319) to transfer the designed mask pattern onto the photoresist. I then cleaned it with deionized water and blow dry with nitrogen gas.

3.4 Permalloy Growth

I mounted the photolithographically patterned sample onto a bracket and installed it in the sputtering system (MiniLab 60) to deposit permalloy into the patterned hollow structures. Firstly, I started the vacuum system and extracted the gas from the system to achieve a required vacuum environment. It was usually necessary to extract the gas to a good vacuum level to avoid the influence of impurities such as oxygen on the sputtering process.

I set the deposition parameters once the vacuum reached around 5×10^{-6} mbar. Firstly, I set the density to 8.9 g/cm^3 and the rotation speed to 0.5 r/s. The Ar gas flow rate was set to 1 sccm then Ar gas was introduced into the system until the Ar gas pressure reaches 0.01mbar.

Afterwards, DC magnetron sputtering was used at the sputtering power of 120 W and running for about 15 minutes to remove surface impurities while keeping the sample baffle closed. I then set the power to 105 W and wait for the plasma glow to be stabilized

to open the baffle. The sputtering rate was monitored during the process to be 0.4-0.5 nm/s. The total thickness I sputtered was about 2 μm, which was broken into four sets of 500 nm thick sputtering to minimize the damage induced on the resist, At the end of each set, I stopped the output power to the target for about 15 minutes. The start and end of sputtering was controlled through a baffle. After the entire sputtering process, the sample was taken out from the chamber and lifted-off using photoresist remover (1165) and isopropanol to finally obtain the permalloy dots.

The dots were imaged using an optical microscope to evaluate the shape and the radius of the dots to find the best deposition condition and diameter to form hemispheres.

3.5 Four-terminal Measurements

A four-terminal method is a commonly used low resistance measurement technique. It is well known that wire and contact resistance can affect the measurement of low resistance values. Unlike a two-terminal method, the four-terminal method can avoid the influence of both parasitic resistance.

Figure 3.6 is the circuit diagram of the two-terminal method. $R3$ and $R4$ are the measured wire resistance, $R7$ and $R8$ are the contact resistance between the wire and the measured resistance $R11$. The voltage measured by the voltmeter is U, and the current flowing through the constant current source is I, satisfying the relationship, $U = I \times (R3 + R4 + R7 + R8 + R11)$. Therefore, it can be seen that when the two-terminal method is used for measurement, the wire and contact resistance can be superimposed. When the magnitude of the measured resistance $R11$ is small, the error in the measurement becomes large.

Figure 3.7 is the circuit diagram of the four-terminal method. The internal resistance of the voltmeter is Ri, the measured wire resistance are $R5$ and $R6$, the contact resistance are $R9$ and $R10$, and the measured resistance is $R12$, For the measurement, Ia is the constant current source current, and Ib is the current flowing through the voltmeter. The voltage at both ends of the measured resistor $R12$ can be defined as

$$U = I\text{b} \times (R5 + R9 + R\text{i} + R6 + R10) = (I\text{a} - I\text{b}) \times R12$$

The displayed value of the voltmeter is accordingly calculated as $U1 = I\text{b} \times R\text{i}$. Due to

$Ri >> R5 + R9 + R6 + R10$, $Ia >> Ib$, Hence $U1 = Ib \times Ri = Ia \times R12$.

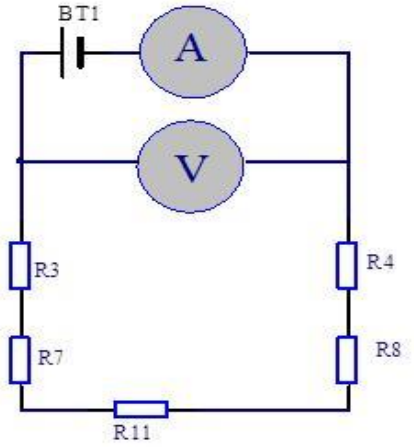

Figure 3.6 Two-terminal method.

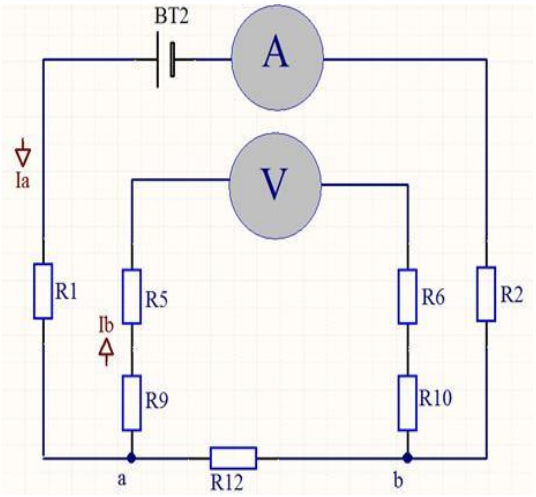

Figure 3.7 Four-terminal method.

Notes:BT_1 and BT_2 are power source that used to inject spin current.

A is used to measure current. V is used to measure voltage.

The four-terminal method is particularly useful when accurate and reliable measurements of resistance or resistivity are required, especially for low-resistance samples where contact resistances can be comparable to the sample resistance. This technique is widely used in both research and industry for material characterization and quality control in manufacturing electronic devices.

4. Results and Discussion

After the experiment, I obtained my sample, but the permalloy dots on it were not perfectly hemispherical, but more like cylindrical shapes.

Although I have designed various diameters on the mask, the actual one that can be used is only 1.5 μ m. 2 μm,2.5 μm,3 μm,3.5 μm,4 μm.

Because the minimum accuracy of the company can only reach 1μm. So it leads to the circles that diameter are 1 μm are not very clear.(see Figure 4.1)

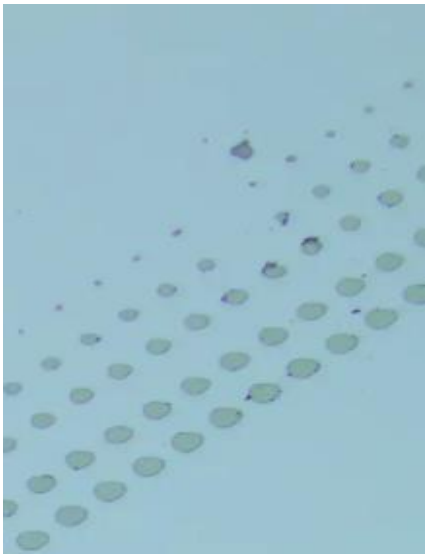

Figure 4.1

The optimal thickness of photoresist is approximately 2 μm. In order to achieve a semi circular effect, the selection of the maximum diameter cannot exceed 4 μm.

Meanwhile, larger diameter dots will cause adjacent dots to connect together during the sputtering. (see Figure 4.2)

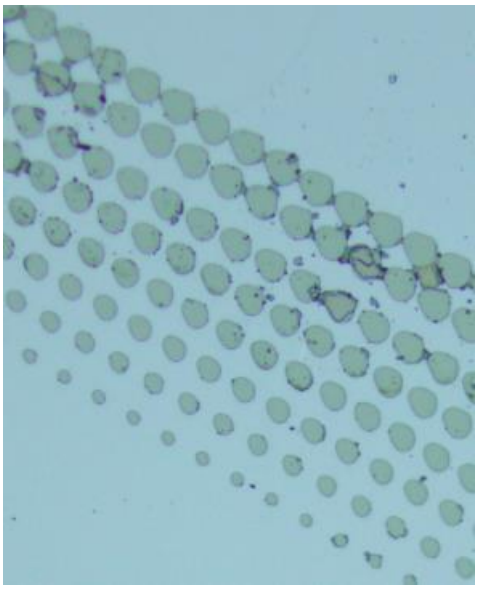

Figure 4.2

In photolithography, it is found that the photolithography effect is influenced by time and power. A short exposure time can lead to incomplete shape, while a long exposure time can cause changes in shape and size. In order to achieve better shape and structure, it is necessary to continuously optimize exposure time and power in practice to achieve better results.(see Figure 4.3)

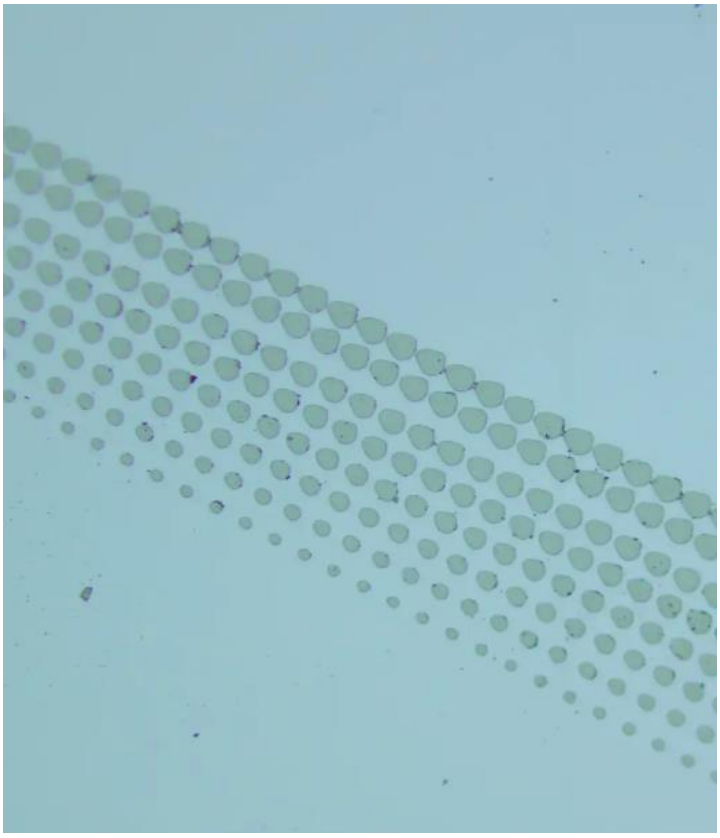

Figure 4.3

At the same time, the development time can also affect the lithography effect. When other conditions are the same, an excessively long development time can make the edges appear like steps, and a perfect development edge should be vertical.

During the sputtering process, I found that using magnetic materials as targets in DC sputtering can affect the production of plasma in the sputtering system. Thinner targets are more easily excited.

In the experiment, we tried 1/4,1/8 and 1/16 inch permalloy targets respectively, and only 1/16 inch had the best result, getting the plasma. Due to the majority of magnetic field lines passing through the interior of the magnetic material, the surface magnetic field of the target decreases, requiring a higher voltage to excite the target. By observing the samples obtained after sputtering, the different incidence angle between the substrate and the position beam did not significantly contribute to the formation of a hemispherical shape, but had some impact on the thickness.

5. Conclusion and Future Persectives

Due to the malfunction of the probe station in the Department of Electronic Engineering, I did not perform any measurements of spin Hall effect or non-local measurement. Due to the very small size of my sample, I was unable to find an alternative instrument for measurement.

I didn't get any data on spin diffusion length so that I don't have data to analyze and obtain any conclusions about spin transport.

References

[1]C. T. Sebens, “How electrons spin,” Nov. 01, 2019. doi:10.1016/j.shpsb.2019.04.007

[2]G. Dosi and L. Galambos, *The Third Industrial Revolution in Global Business*. Cambridge University Press, 2013. http://books.google.ie/books?id=FAUsthoSdAQC&printsec=frontcover&dq=The+Third+Industrial+Revolution+in+Global+Business&hl=&cd=1&source=gbs_api

[3]“An Industry Perspective on Current and Future State of the Art in System-on-Chip (SoC) Technology,” *IEEE Journals & Magazine | IEEE Xplore*, Jun. 01, 2006. https://ieeexplore.ieee.org/abstract/document/1652901

[4]“Electrical-Thermal Co-Simulation of 3D Integrated Systems With Micro-Fluidic Cooling and Joule Heating Effects,” *IEEE Journals & Magazine | IEEE Xplore*, Feb. 01, 2011. https://ieeexplore.ieee.org/abstract/document/5699963

[5]J. W. Lu, E. Chen, M. Kabir, M. R. Stan, and S. A. Wolf, “Spintronics technology: past, present and future,” *International Materials Reviews*, vol. 61, no. 7, pp. 456–472, Jul. 2016, doi: 10.1080/09506608.2016.1204097.

[6]S. A. Wolf *et al.*, “Spintronics: A Spin-Based Electronics Vision for the Future,” *Science*, vol. 294, no. 5546, pp. 1488–1495, Nov. 2001, doi:10.1126/science.1065389.

[7]D. D. Awschalom, M. E. Flatté, and N. Samarth, “Spintronics,” *Scientific American*, vol. 286, no. 6, pp. 66–73, Jun. 2002, doi: 10.1038/scientificamerican0602-66.

[8]W. Wu, “Stretchable electronics: functional materials, fabrication strategies and applications,” *Science and Technology of Advanced Materials*, vol. 20, no. 1, pp. 187–224, Mar. 2019, doi: 10.1080/14686996.2018.1549460.

[9]Z. Zhen and H. Zhu, “Structure and Properties of Graphene,” *Elsevier eBooks*, Jan. 01, 2018. doi: 10.1016/b978-0-12-812651-6.00001-x

[10]T. C. Dinadayalane and J. Leszczyński, “Remarkable diversity of carbon–carbon bonds: structures and properties of fullerenes, carbon nanotubes, and graphene,” *Structural Chemistry*, Nov. 09, 2010. doi: /10.1007/s11224-010-9670-2

[11]N. K. Mahanta, A. R. Abramson, and J. Y. Howe, “Thermal conductivity measurements on individual vapor-grown carbon nanofibers and graphene nanoplatelets,” Journal of Applied Physics, Oct. 28, 2013. doi: 10.1063/1.4827378

[12]A. Nieto, D. Lahiri, and A. Agarwal, “Graphene NanoPlatelets reinforced tantalum carbide consolidated by spark plasma sintering,” *Materials Science and Engineering: A*, Oct. 01, 2013. doi: 10.1016/j.msea.2013.06.006

[13]X. Cai, First Principle-based Research On Properties of Twisted Bilayer of Graphene and GaN. Swansea, 2021. doi:10.23889/SUthesis.58747

[14]Y. Wu, D. B. Farmer, F. Xia, and P. Avouris, “Graphene Electronics: Materials, Devices, and Circuits,” *Proceedings of the IEEE*, vol. 101, no. 7, pp. 1620–1637, Jul. 2013, doi: 10.1109/jproc.2013.2260311.

[15] Seneor P, Dlubak B, Martin M-B, Anane A, Jaffres H, Fert A. Spintronics with graphene. *MRS Bulletin*. 2012;37(12):1245-1254. doi:10.1557/mrs.2012.277

[16]Z. Tang *et al.*, “Dynamically generated pure spin current in single-layer graphene,” *Physical Review B*, Apr. 02, 2013. doi: 10.1103/physrevb.87.140401

[17]W. Han, R. Kawakami, M. Gmitra, and J. Fabian, “Graphene spintronics,” *Nature Nanotechnology*, Oct. 01, 2014. doi: 10.1038/nnano.2014.214

[18]C. Guan *et al.*, “Pseudospin-Mediated Optical Spin–Spin Interaction in Nonlinear Photonic Graphene,” *Laser & Photonics Reviews*, vol. 13, no. 2, Nov. 2018, doi: 10.1002/lpor.201800242.

[19]W. Han *et al.*, “Spin transport and relaxation in graphene,” *Journal of Magnetism and Magnetic Materials*, Feb. 01, 2012. doi: /10.1016/j.jmmm.2011.08.001

[20]S. Takahashi and S. Maekawa, “Spin current, spin accumulation and spin Hall effect,” *Science and Technology of Advanced Materials*, vol. 9, no. 1, p. 014105, Jan. 2008, doi: 10.1088/1468-6996/9/1/014105.

[21]W.-T. Lu, “Valley-dependent band structure and valley polarization in periodically modulated graphene,” *Physical Review B*, vol. 94, no. 8, Aug. 2016, doi: 10.1103/physrevb.94.085403.

[22]Y.-T. Chen *et al.*, “Theory of spin Hall magnetoresistance,” *Physical Review B*, vol. 87, no. 14, Apr. 2013, doi: 10.1103/physrevb.87.144411.

[23]I. P. Smorchkova, F. S. Flack, N. Samarth, J. M. Kikkawa, S. A. Crooker, and D. D. Awschalom, “Spin transport and optically-probed coherence in magnetic semiconductor heterostructures,” *Physica B: Condensed Matter*, vol. 249–251, pp. 676–684, Jun. 1998, doi: 10.1016/s0921-4526(98)00288-9.

[24]F. Pei, E. A. Laird, G. A. Steele, and L. P. Kouwenhoven, “Valley–spin blockade and spin resonance in carbon nanotubes,” *Nature Nanotechnology*, vol. 7, no. 10, pp. 630–634, Sep. 2012, doi: 10.1038/nnano.2012.160.

[25]C.-N. Ahn, “2D materials for spintronic devices,” *npj 2D Materials and Applications*, Jun. 18, 2020. https://doi.org/10.1038/s41699-020-0152-0

[26]E. W. Hill, A. K. Geim, K. Novoselov, F. Schedin, and P. Blake, “Graphene Spin Valve Devices,” *IEEE Transactions on Magnetics*, vol. 42, no. 10, pp. 2694–2696, Oct. 2006, doi: 10.1109/tmag.2006.878852.

[27]M. Drögeler *et al.*, “Nanosecond Spin Lifetimes in Single- and Few-Layer Graphene–hBN Heterostructures at Room Temperature,” *Nano Letters*, vol. 14, no. 11, pp. 6050–6055, Oct. 2014, doi: 10.1021/nl501278c.

[28]M. Saeed, Y. Alshammari, S. A. Majeed, and E. Al-Nasrallah, “Chemical Vapour Deposition of Graphene—Synthesis, Characterisation, and Applications: A Review,” *Molecules*, Aug. 25, 2020. https://doi.org/10.3390/molecules25173856

[29]. Avsar *et al.*, “Toward Wafer Scale Fabrication of Graphene Based Spin Valve Devices,” *Nano Letters*, vol. 11, no. 6, pp. 2363–2368, May 2011, doi: 10.1021/nl200714q.

[30]P. R. Wallace, “The Band Theory of Graphite,” *Physical Review*, vol. 71, no. 9, pp. 622–634, May 1947, doi: 10.1103/physrev.71.622.

[31]D. S. L. Abergel, V. Apalkov, J. Berashevich, K. Ziegler, and T. Chakraborty, “Properties of graphene: a theoretical perspective,” *Advances in Physics*, vol. 59, no. 4, pp. 261–482, Jul. 2010, doi: 10.1080/00018732.2010.487978.

[32]K. S. Novoselov *et al.*, “Two-dimensional gas of massless Dirac fermions in graphene,” *Nature*, vol. 438, no. 7065, pp. 197–200, Nov. 2005, doi: 10.1038/nature04233.

[33]K. I. Bolotin *et al.*, “Ultrahigh electron mobility in suspended graphene,” *Solid State Communications*, vol. 146, no. 9–10, pp. 351–355, Jun. 2008, doi: 10.1016/j.ssc.2008.02.024.

[34]C. R. Dean *et al.*, “Boron nitride substrates for high-quality graphene electronics,” *Nature Nanotechnology*, vol. 5, no. 10, pp. 722–726, Aug. 2010, doi: 10.1038/nnano.2010.172.

[35]T. Ohta, A. Bostwick, T. Seyller, K. Horn, and E. Rotenberg, “Controlling the Electronic Structure of Bilayer Graphene,” *Science*, vol. 313, no. 5789, pp. 951–954, Aug. 2006, doi: 10.1126/science.1130681.

[36]J. B. Oostinga, H. B. Heersche, X. Liu, A. F. Morpurgo, and L. M. K. Vandersypen, “Gate-induced insulating state in bilayer graphene devices,” *Nature Materials*, vol. 7, no. 2, pp. 151–157, Dec. 2007, doi: 10.1038/nmat2082.

[37]G. Fiori and G. Iannaccone, “Ultralow-Voltage Bilayer Graphene Tunnel FET,” *IEEE Electron Device Letters*, vol. 30, no. 10, pp. 1096–1098, Oct. 2009, doi: 10.1109/led.2009.2028248.

[38]“XIX. On the electro-dynamic qualities of metals:—Effects of magnetization on the electric conductivity of nickel and of iron,” *Proceedings of the Royal Society of London*, vol. 8, pp. 546–550, Dec. 1857, doi: 10.1098/rspl.1856.0144.

[39]B. Heinrich and J. A. C. Bland, *Ultrathin Magnetic Structures II*. Springer Science & Business Media, 2005.page 198-296.

[40]A. Berkowitz and W. Meiklejohn, “Thermomagnetic recording: Physics and materials,” *IEEE Transactions on Magnetics*, vol. 11, no. 4, pp. 996–1017, Jul. 1975, doi: 10.1109/tmag.1975.1058780.

[41]P. Grünberg, R. Schreiber, Y. Pang, M. B. Brodsky, and H. Sowers, “Layered Magnetic Structures: Evidence for Antiferromagnetic Coupling of Fe Layers across Cr Interlayers,” *Physical Review Letters*, vol. 57, no. 19, pp. 2442–2445, Nov. 1986, doi: 10.1103/physrevlett.57.2442.

[42]M. N. Baibich *et al.*, “Giant Magnetoresistance of(001)Fe/(001)Cr Magnetic Superlattices,” *Physical Review Letters*, vol. 61, no. 21, pp. 2472–2475, Nov. 1988, doi: 10.1103/physrevlett.61.2472.

[43]B. Dieny, V. S. Speriosu, S. S. P. Parkin, B. A. Gurney, D. R. Wilhoit, and D. Mauri, “Giant magnetoresistive in soft ferromagnetic multilayers,” *Physical Review B*, vol. 43, no. 1, pp. 1297–1300, Jan. 1991, doi: 10.1103/physrevb.43.1297.

[44]G. Binasch, P. Grünberg, F. Saurenbach, and W. Zinn, “Enhanced magnetoresistance in layered magnetic structures with antiferromagnetic interlayer exchange,” *Physical Review B*, vol. 39, no. 7, pp. 4828–4830, Mar. 1989, doi: 10.1103/physrevb.39.4828.

[45]M. Sato, H. Kikuchi, and K. Kobayashi, “Ferromagnetic tunnel junctions with plasma-oxidized Al barriers and their annealing effects,” *Journal of Applied Physics*, vol. 83, no. 11, pp. 6691–6693, Jun. 1998, doi: 10.1063/1.367933.

[46]S. S. P. Parkin *et al.*, “Giant tunnelling magnetoresistance at room temperature with MgO (100) tunnel barriers,” *Nature Materials*, vol. 3, no. 12, pp. 862–867, Oct. 2004, doi: 10.1038/nmat1256.

[47]S. A. Wolf *et al.*, “Spintronics: A Spin-Based Electronics Vision for the Future,” *Science*, vol. 294, no. 5546, pp. 1488–1495, Nov. 2001, doi: 10.1126/science.1065389.

[48]Aronov, A. G., and G. E. Pikus. "Spin injection into semiconductors." Soviet Physics Semiconductors-Ussr 10, no. 6 (1976): 698-700.

[49]S. Takahashi and S. Maekawa, “Spin Current in Metals and Superconductors,” *Journal of the Physical Society of Japan*, vol. 77, no. 3, p. 031009, Mar. 2008, doi: 10.1143/jpsj.77.031009.

[50]M. Johnson and R. H. Silsbee, “Interfacial charge-spin coupling: Injection and detection of spin magnetization in metals,” *Physical Review Letters*, vol. 55, no. 17, pp. 1790–1793, Oct. 1985, doi: 10.1103/physrevlett.55.1790.

[51]F. J. Jedema, A. T. Filip, and B. J. van Wees, “Electrical spin injection and accumulation at room temperature in an all-metal mesoscopic spin valve,” *Nature*, vol. 410, no. 6826, pp. 345–348, Mar. 2001, doi: 10.1038/35066533.

[52]E. I. Rashba, “Theory of electrical spin injection: Tunnel contacts as a solution of the conductivity mismatch problem,” *Physical Review B*, vol. 62, no. 24, pp. R16267–R16270, Dec. 2000, doi: 10.1103/physrevb.62.r16267.

[53]S. Hershfield and H. L. Zhao, “Charge and spin transport through a metallic ferromagnetic-paramagnetic-ferromagnetic junction,” *Physical Review B*, vol. 56, no. 6, pp. 3296–3305, Aug. 1997, doi: 10.1103/physrevb.56.3296.

[54]S. Takahashi and S. Maekawa, “Spin injection and detection in magnetic nanostructures,” *Physical Review B*, vol. 67, no. 5, Feb. 2003, doi: 10.1103/physrevb.67.052409.

[55]T. Kimura, J. Hamrle, and Y. Otani, “Estimation of spin-diffusion length from the magnitude of spin-current absorption: Multiterminal ferromagnetic/nonferromagnetic hybrid structures,” *Physical Review B*, vol. 72, no. 1, Jul. 2005, doi: 10.1103/physrevb.72.014461.

[56]S. O. Valenzuela and M. Tinkham, “Direct electronic measurement of the spin Hall effect,” *Nature*, vol. 442, no. 7099, pp. 176–179, Jul. 2006, doi: 10.1038/nature04937.

[57]Y. Fukuma, L. Wang, H. Idzuchi, S. Takahashi, S. Maekawa, and Y. Otani, “Giant enhancement of spin accumulation and long-distance spin precession in metallic lateral spin valves,” *Nature Materials*, vol. 10, no. 7, pp. 527–531, Jun. 2011, doi: 10.1038/nmat3046.

[58]Dyakonov, Mikhail I and V. I. Perel. ,"Possibility of orienting electron spins with current." JETP Lett. USSR 13 (1971): 467.

[59]Y. Niimi et al., “Giant Spin Hall Effect Induced by Skew Scattering from Bismuth Impurities inside Thin Film CuBi Alloys,” Physical Review Letters, vol. 109, no. 15, Oct. 2012, doi: 10.1103/physrevlett.109.156602.

[60]S. Murakami, N. Nagaosa, and S.-C. Zhang, “Dissipationless Quantum Spin Current at Room Temperature,” Science, vol. 301, no. 5638, pp. 1348–1351, Sep. 2003, doi: 10.1126/science.1087128.

[61]S. Zhang, “Spin Hall Effect in the Presence of Spin Diffusion,” Physical Review Letters, vol. 85, no. 2, pp. 393–396, Jul. 2000, doi: 10.1103/physrevlett.85.393.

[62]S. Murakami, “Absence of vertex correction for the spin Hall effect inp-type semiconductors,” Physical Review B, vol. 69, no. 24, Jun. 2004, doi: 10.1103/physrevb.69.241202.

[63]J. Sinova, D. Culcer, Q. Niu, N. A. Sinitsyn, T. Jungwirth, and A. H. MacDonald, “Universal Intrinsic Spin Hall Effect,” Physical Review Letters, vol. 92, no. 12, Mar. 2004, doi: 10.1103/physrevlett.92.126603.

[64]Y. K. Kato, R. C. Myers, A. C. Gossard, and D. D. Awschalom, “Observation of the Spin Hall Effect in Semiconductors,” Science, vol. 306, no. 5703, pp. 1910–1913, Dec. 2004, doi: 10.1126/science.1105514.

[65]J. Wunderlich, B. Kaestner, J. Sinova, and T. Jungwirth, “Experimental Observation of the Spin-Hall Effect in a Two-Dimensional Spin-Orbit Coupled Semiconductor System,” Physical Review Letters, vol. 94, no. 4, Feb. 2005, doi: 10.1103/physrevlett.94.047204.

[66]C. L. Kane and E. J. Mele, “Quantum Spin Hall Effect in Graphene,” Physical Review Letters, vol. 95, no. 22, Nov. 2005, doi: 10.1103/physrevlett.95.226801.

[67]B. A. Bernevig, T. L. Hughes, and S.-C. Zhang, “Quantum Spin Hall Effect and Topological Phase Transition in HgTe Quantum Wells,” Science, vol. 314, no. 5806, pp. 1757–1761, Dec. 2006, doi: 10.1126/science.1133734.

[68]M. König et al., “Quantum Spin Hall Insulator State in HgTe Quantum Wells,” Science, vol. 318, no. 5851, pp. 766–770, Nov. 2007, doi: 10.1126/science.1148047.

[69]R. Yu, W. Zhang, H.-J. Zhang, S.-C. Zhang, X. Dai, and Z. Fang, “Quantized Anomalous Hall Effect in Magnetic Topological Insulators,” Science, vol. 329, no. 5987, pp. 61–64, Jul. 2010, doi: 10.1126/science.1187485.

[70]C.-Z. Chang et al., “Experimental Observation of the Quantum Anomalous Hall Effect in a Magnetic Topological Insulator,” Science, vol. 340, no. 6129, pp. 167–170, Apr. 2013, doi: 10.1126/science.1234414.

[71] M. Drögeler et al., “Spin Lifetimes Exceeding 12 ns in Graphene Nonlocal Spin Valve Devices,” Nano Letters, vol. 16, no. 6, pp. 3533–3539, May 2016, doi: 10.1021/acs.nanolett.6b00497.